Contribution from the Department of Chemistry,
The University of Texas at Arlington, Arlington, Texas 76019-0065

# Relationships between Bonding and Structure in Tetranuclear Heteroatomic Zintl Anions Containing 20 Valence Electrons

Frank U. Axe and Dennis S. Marynick*

*Received July 27, 1987*

The SW-X$\alpha$ method employing quasi-relativistic corrections was used to study the bonding in the 20-electron tetranuclear heteroatomic Zintl anions $Sn_2Bi_2^{2-}$, $Pb_2Sb_2^{2-}$ and $Tl_2Te_2^{2-}$. The electronic structure of the classically bonded, tetrahedrally shaped $Sn_2Bi_2^{2-}$ and $Pb_2Sb_2^{2-}$ anions is best described as being very covalent in nature. The bonding molecular orbitals (MO's) in these two anions are formed almost exclusively from the valence p atomic orbitals (AO's). The localized valence structure is consistent with six two-center, two-electron bonds located along the edges of the tetrahedron with an inner-shell lone pair residing on each atom. The lowest unoccupied MO in the two classically bonded anions is based primarily on the more electronegative atoms and is antibonding with respect to them. The $Tl_2Te_2^{2-}$ anion has a nonclassical structure, which can be described as an open "boat" or "butterfly" geometry. The bonding in this species is best described as the coordination of two $Te^{2-}$ anions by two $Tl^+$ cations. The localized valence structure requires four bonds; however, only three bonding MO's are found. Each Te atom has a $5p_\pi$ lone-pair orbital, which occupies a stereochemical position in the coordination sphere of the atoms. These two lone-pair orbitals repel one another and are responsible for the Te-Te distance being longer than the Tl-Tl distance. In addition each atom has an inner-shell lone pair, which has predominantly atomic s character. Since the $Tl_2Te_2^{2-}$ anion is very ionic, its structure should be planar, but in reality it is puckered. A repulsive interaction between the antisymmetric combination of the Tl 6s AO's and an occupied Te 5p based MO of the same symmetry is responsible for this distortion from the plane geometry.

## Introduction

There is a growing interest in the synthesis, detection, isolation, and structural characterization of numerous homopolyatomic (i.e. $Ge_9^{4-}$,[2] $Sn_9^{4-}$,[3] $Sn_5^{2-}$,[4] $Pb_5^{2-}$,[4] $Sn_4^{2-}$,[5] $As_{11}^{3-}$,[6] $Te_3^{2-}$,[7] $Sb_4^{2-}$,[8] $Sb_7^{2-}$,[8] $Bi_4^{2-}$[9]) and heteropolyatomic (i.e. $HgTe_2^{2-}$,[10,11] $HgSe_2^{2-}$,[11] $Sn_2Bi_2^{2-}$,[12] $Pb_2Sb_2^{2-}$,[13] $Tl_2Te_2^{2-}$,[11,14] $Tl_2Se_2^{2-}$,[11] $TlSn_9^{2-}$,[15] $As_2Se_6^{2-}$,[16] $Pb_2Te_3^{2-}$,[17] $Pb_2Se_3^{2-}$[17]) Zintl anions. Structural studies of these species have provided the most useful information with regard to the arrangement and connectivity of the constituent atoms involved. As a result of this structural work it is now known that many Zintl anions are analogous to many better known compounds composed of first- and second-row atoms. For instance, homopolyatomic anions like $Sn_4^{4-}$,[18] $Pb_4^{4-}$,[19] and $Tl_4^{8-}$[20] all have tetrahedral structures and also possess a complement of 20 valence electrons. These species are believed to have bonding traits similar to those of the more widely known $P_4$, $As_4$, and $Sb_4$ molecules, which also have tetrahedral structures. Another more intriguing analogy has been made[1a] between the $Sn_5^{2-}$ and $Pb_5^{2-}$ anions and $B_5H_5^{2-}$ and $B_4CH_5^-$. Other analogies have also been cited.[1] Due to the broader definition[21,22] of the term "cluster", many Zintl anions are representatives of these kinds of species.

In spite of the wealth of experimental studies on Zintl anions, only a limited understanding of the bonding in these systems exists at present. Much of the bonding in these systems is believed[1,23] to occur through the valence p atomic orbitals (AO's), while the valence s AO's remain doubly occupied and are inert. For instance, the $^1J$ coupling constants in $Pb_2Se_3^{2-}$ and $Pb_2Te_3^{2-}$ have been shown to be consistent with bonding largely through valence p orbitals.[17] Several existing electron-counting schemes have been used to treat the bonding in polyanions.[22] Unfortunately, none of these valence rules can be applied to describing and/or predicting the bonding in all kinds of Zintl anions. Consequently, there is a definite need for the application of first-principle approaches to the study of these species. Presently, only a handful of quantum-mechanical studies[2,24,25] on Zintl anions exist in the literature. These studies have focused primarily upon conformational preferences and potential fluctionality in predominantly homopolyatomic Zintl anions. In contrast, very little attention has been devoted to describing the modes of bonding present in these systems, especially for the heteropolyatomic species.

Some of the more interesting heteropolyatomic Zintl anions are $Sn_2Bi_2^{2-}$, $Pb_2Sb_2^{2-}$, and $Tl_2Te_2^{2-}$. All three anions have been structurally characterized.[12-14] Both $Sn_2Bi_2^{2-}$[12] and $Pb_2Sb_2^{2-}$[13] have tetrahedral structures. Each of these anions has a complement of 20 valence electrons and therefore might be construed as being analogous to the $P_4$ family of molecules. Oddly enough, $Tl_2Te_2^{2-}$[14] does not adhere to the 20-electron tetrahedral structural convention but has an open "boat" or "butterfly" geometry. Several explanations of this geometric anomaly have been discussed.[14,25] First, one might consider[14] the $Tl_2Te_2^{2-}$ anion to have a structure that is intermediate to the tetrahedral geometries of typical 20-electron systems and the square-planar $D_{4h}$ geometries of 22-electron tetraatomic systems like $Sb_4^{2-}$[8] and $Bi_4^{2-}$.[9] These systems are generally considered to be 6-$\pi$-electron quasi-aromatic species. The $Tl_2Te_2^{2-}$ anion, which has only 20 valence electrons, would have a 4-$\pi$-electron system; however, this is not an apparent violation of the Hückel rule. Due to the $C_{2v}$ symmetry of the anion, the 4-$\pi$-electron system is allowed and should consist of a bonding $a_1$ MO and a nonbonding $b_1$ or $b_2$ MO. Alternatively, the departure of the $Tl_2Te_2^{2-}$ anion's structure from the norm may be attributed to the large periodic displacement of the Tl and Te

(1) (a) Corbett, J. D. *Chem. Rev.* **1985**, *85*, 383. (b) Corbett, J. D. In *Chemistry for the Future*; Grunewald, H., Ed.; Pergamon: Oxford, UK, 1984; p 125. (c) Corbett, J. D.; Critchlow, S. C.; Burns, R. C. *ACS Symp. Ser.* **1983**, *No. 232*, 95.
(2) Belin, C. H. E.; Corbett, J. D.; Cisar, A. *J. Am. Chem. Soc.* **1977**, *99*, 7163.
(3) Corbett, J. D.; Edwards, P. A. *J. Am. Chem. Soc.* **1977**, *99*, 3313.
(4) Edwards, P. A.; Corbett, J. D. *Inorg. Chem.* **1977**, *16*, 903.
(5) Rudolph, R. W.; Wilson, W. L.; Taylor, R. C. *J. Am. Chem. Soc.* **1981**, *103*, 2480.
(6) Belin, C. H. E. *J. Am. Chem. Soc.* **1980**, *102*, 6036.
(7) Cisar, A.; Corbett, J. D. *Inorg. Chem.* **1977**, *16*, 632.
(8) Critchlow, S. C.; Corbett, J. D. *Inorg. Chem.* **1984**, *23*, 770.
(9) Cisar, A.; Corbett, J. D. *Inorg. Chem.* **1977**, *16*, 2482.
(10) Burns, R. C.; Corbett, J. D. *Inorg. Chem.* **1981**, *20*, 4433.
(11) Burns, R. C.; Devereux, L. A.; Granger, P.; Schrobilgen, G. J. *Inorg. Chem.* **1985**, *24*, 2615.
(12) Critchlow, S. C.; Corbett, J. D. *Inorg. Chem.* **1982**, *21*, 3286.
(13) Critchlow, S. C.; Corbett, J. D. *Inorg. Chem.* **1985**, *24*, 979.
(14) Burns, R. C.; Corbett, J. D. *J. Am. Chem. Soc.* **1981**, *103*, 2627.
(15) Burns, R. C.; Corbett, J. D. *J. Am. Chem. Soc.* **1982**, *104*, 2804.
(16) Belin, C. H. E.; Charbonnel, M. M. *Inorg. Chem.* **1982**, *21*, 2504.
(17) Björgvinsson, M.; Sawyer, J. F.; Schrobilgen, G. J. *Inorg. Chem.* **1987**, *26*, 741.
(18) Hewaidy, I. F.; Busmann, E.; Klemm, W. *Z. Anorg. Allg. Chem.* **1964**, *328*, 283.
(19) Marsh, R. E.; Shoemaker, D. P. *Acta Crystallogr.* **1953**, *6*, 197.
(20) Hansen, D. A.; Smith, J. F. *Acta Crystallogr.* **1967**, *22*, 836.
(21) Martin, T. P. *Angew. Chem., Int. Ed. Engl.* **1986**, *25*, 197.
(22) von Schnering, H. G. *Angew. Chem., Int. Ed. Engl.* **1981**, *20*, 336.
(23) Corbett, J. D.; Rundle, R. E. *Inorg. Chem.* **1964**, *3*, 1408.
(24) (a) Lohr, L. L. *Inorg. Chem.* **1981**, *20*, 4229. (b) Burns, R. C.; Gillespie, R. J.; Barnes, J. A.; McGlinchey, M. J. *Inorg. Chem.* **1982**, *21*, 799. (c) Rothman, J. M.; Bartell, L. S.; Lohr, L. L. *J. Am. Chem. Soc.* **1981**, *103*, 2482. (d) Wilson, W. L.; Rudolph, R.; Lohr, L. L.; Taylor, R. C.; Pyykkö, P *Inorg. Chem.* **1986**, *25*, 1535.
(25) Axe, F. U.; Marynick, D. S. *Inorg. Chem.* **1987**, *26*, 1658.

0020-1669/88/1327-1426$01.50/0 

**Table I.** Geometrical Parameters, Sphere Radii, and $X\alpha_{HF}$ Values Used in the SW–X$\alpha$ Calculations

| $Sn_2Bi_2^{2-}$ | $Pb_2Sb_2^{2-}$ | $Tl_2Te_2^{2-}$ |
|---|---|---|
| Sn–Sn[a] = 2.870 | Pb–Pb = 3.002 | Tl–Tl = 3.600 |
| Bi–Bi = 3.050 | Sb–Sb = 2.858 | Te–Te = 4.414 |
| Sn–Bi = 2.960 | Pb–Sb = 2.930 | Tl–Te = 2.954 |
| $r_{Sn}$[b] = 3.022 56 | $r_{Pb}$ = 3.116 13 | $r_{Tl}$ = 3.176 57 |
| $r_{Bi}$ = 3.159 23 | $r_{Sb}$ = 3.003 53 | $r_{Te}$ = 3.168 17 |
| $r_{out}$ = 6.534 59 | $r_{out}$ = 6.690 29 | $r_{out}$ = 7.368 10 |
| $\alpha_{Sn}$[c] = 0.700 78 | $\alpha_{Pb}$ = 0.692 81 | $\alpha_{Tl}$ = 0.692 89 |
| $\alpha_{Bi}$ = 0.692 72 | $\alpha_{Sb}$ = 0.700 55 | $\alpha_{Te}$ = 0.700 31 |
| $\alpha_{int,out}$ = 0.696 30 | $\alpha_{int,out}$ = 0.697 11 | $\alpha_{int,out}$ = 0.697 84 |

[a] Internuclear distances (Å). [b] Atomic and outer-sphere radii (bohr). [c] X$\alpha$ exchange parameters.

atoms, leading to a significant ionic component to the bonding. This was found to be the case in our recent theoretical analysis[25] of the $HgTe_2^{2-}$ anion. The $Sn_2Bi_2^{2-}$ and $Pb_2Sb_2^{2-}$ anions both contain atoms that are very close to one another periodically; therefore, the bonding appears to be covalent as in the $P_4$ molecule. It is not at all clear which rationale is more appropriate for describing the bonding in $Tl_2Te_2^{2-}$. For these reasons we have undertaken a theoretical study of the bonding present in $Sn_2Bi_2^{2-}$, $Pb_2Sb_2^{2-}$, and $Tl_2Te_2^{-}$.

In an effort to elucidate the important features of the bonding present in these anions, we present scattered-wave (SW) X$\alpha$ self-consistent-field (SCF) calculations on the $Sn_2Bi_2^{2-}$, $Pb_2Sb_2^{2-}$, and $Tl_2Te_2^{2-}$ anions.[10-14] A particular emphasis will be placed upon understanding the electronic differences between the classically bonded ($Sn_2Bi_2^{2-}$, $Pb_2Sb_2^{2-}$) and the nonclassically bonded ($Tl_2Te_2^{2-}$) anions. The details of the bonding will be discussed with the aid of MO populations, MO energy level diagrams, and wave function contour plots.

## Calculations and Geometries

Spin-restricted scattered-wave X$\alpha$ calculations based upon the method developed originally by Johnson[26] and Slater[27] were performed on the $Sn_2Bi_2^{2-}$, $Pb_2Sb_2^{2-}$, and $Tl_2Te_2^{2-}$ anions.[10-14] Both nonrelativistic and quasi-relativistic[28] calculations were carried out. The geometries of the anions were constructed from the experimental X-ray structures.[12-14] Actual distances used in the SW–X$\alpha$ calculations are reported in Table I. Since each anion has $C_{2v}$ symmetry, the orientation of the molecular clusters in all of our calculations was chosen such that the $z$ axis coincided with the major rotation axis. The more electropositive atoms (Sn, Pb, and Tl) were situated in the $yz$ plane, making the more electronegative atoms (Bi, Sb, and Te) reside in the $yz$ plane. These orientations will be crucial to the development of bonding arguments and the classification of MO symmetry types in the Discussion. The initial molecular potential was formed from the superposition of the neutral free atom Herman–Skillman atomic SCF charge densities. Atomic sphere sizes were taken as 89% of the atomic number radius in accordance with the Norman criterion.[29] The outer spheres were centered at the valence electron weighted average of the atomic positions in each anion with radii that made them tangent to the outermost atomic sphere. The actual sphere sizes used in the calculations are reported in Table I. The $\alpha$ values used in the atomic regions of each anion were taken directly or linearly interpolated from the $\alpha_{HF}$ values obtained by Schwarz.[30] The $\alpha$ values for the inner- and outer-sphere regions for each anion were both taken as a valence electron weighted average of the atomic $\alpha$ values. Wave functions about each atomic sphere were expanded by a set of partial waves that were one "$l$" value higher than the minimal valence representation required for that particular atom (i.e. this corresponded to $l \leq 2$ for Sn, Bi, Pb, Te, and Sb and $l \leq 3$ for Tl). In the $Tl_2Te_2^{2-}$ calculations the Tl 5d AO's were treated as valence electrons. The solutions in the outer-sphere region were expanded in terms of spherical harmonics that were one "$l$" value higher than the highest atomic "$l$" value (i.e. $l \leq 3$ for $Sn_2Bi_2^{2-}$ and $Pb_2Sb_2^{2-}$ and $l \leq 4$ for $Tl_2Te_2^{2-}$). In every calculation a Watson sphere with a charge of +2 was used to provide a more realistic model of the crystalline environment. The Watson spheres were all centered at the same positions and set at the same radius as the outer spheres in each calculation. Each calculation was converged such that the maximum relative change in the molecular potential was less than $10^{-3}$ Ry from one iteration to the next. The nonrelativistic calculations yielded virial ratios[29] (−2T/V) at convergence of 1.000 010, 1.000 013, and 1.000 007 for $Sn_2Bi_2^{2-}$, $Pb_2Sb_2^{2-}$, and $Tl_2Te_2^{2-}$, respectively.

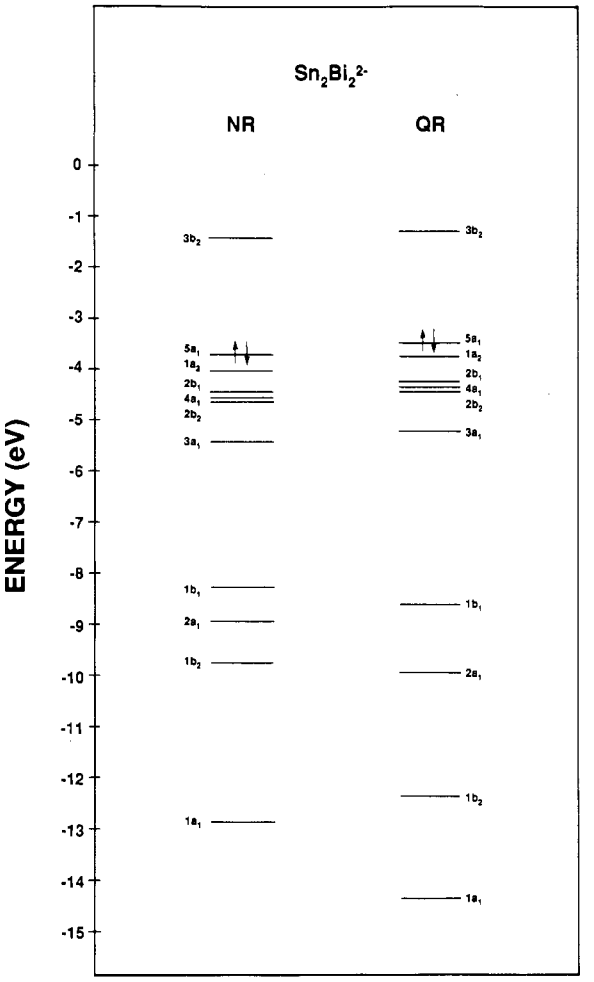


**Figure 1.** MO energy level diagram of the nonrelativistic (NR) and quasi-relativistic (QR) valence ground-state orbital energies (in eV) in the $Sn_2Bi_2^{2-}$ anion.

**Table II.** SW–X$\alpha$ Quasi-Relativistic Muffin-Tin Populations for $Sn_2Bi_2^{2-}$ (%)

| | | Sn | | Bi | | extra-atomic | |
|---|---|---|---|---|---|---|---|
| MO | $-E$[a] | s | p | s | p | int | out |
| $3b_2$ | 1.302 | | 2 | 3 | 41 | 17 | 32 |
| $5a_1$[b] | 3.495 | 0 | 53 | 0 | 10 | 25 | 10 |
| $1a_2$ | 3.764 | | 20 | | 46 | 24 | 8 |
| $2b_1$ | 4.270 | 6 | 21 | | 43 | 21 | 9 |
| $4a_1$ | 4.371 | 4 | 21 | 0 | 45 | 20 | 9 |
| $2b_2$ | 4.461 | | 31 | 1 | 38 | 20 | 7 |
| $3a_1$ | 5.231 | 3 | 21 | 2 | 55 | 6 | 10 |
| $1b_1$ | 8.642 | 73 | 3 | | 8 | 11 | 3 |
| $2a_1$ | 9.960 | 63 | 4 | 15 | 9 | 5 | 2 |
| $1b_2$ | 12.367 | | 2 | 89 | 1 | 5 | 1 |
| $1a_1$ | 14.378 | 14 | 5 | 75 | 4 | 0 | 0 |

[a] MO eigenvalues (eV). [b] Highest occupied MO.

## Discussion

**$Sn_2Bi_2^{2-}$ and $Pb_2Sb_2^{2-}$.** We begin our theoretical analysis with a discussion of the electronic structure of the two classically bonded anions $Sn_2Bi_2^{2-}$ and $Pb_2Sb_2^{2-}$. Presented in Figures 1 and 2 are

(26) (a) Johnson, K. H. *Adv. Quantum Chem.* **1973**, *7*, 143. (b) Johnson, K. H. *Annu. Rev. Phys. Chem.* **1975**, *26*, 39.
(27) Slater, J. C. *Adv. Quantum Chem.* **1972**, *6*, 1.
(28) Wood, J. H.; Boring, A. M. *Phys. Rev. B: Condens. Matter* **1978**, *18*, 2701. The quasi-relativistic corrections are a standard feature of the SW–X$\alpha$ program used, which is the Bursten, Cook, and Case rewrite of the original X$\alpha$ codes.
(29) Norman, J. G. *J. Chem. Phys.* **1974**, *61*, 4630.
(30) (a) Schwarz, K. *Phys. Rev. B: Solid State* **1972**, *5*, 2466. (b) Schwarz, K. *Theor. Chim. Acta* **1974**, *34*, 255.

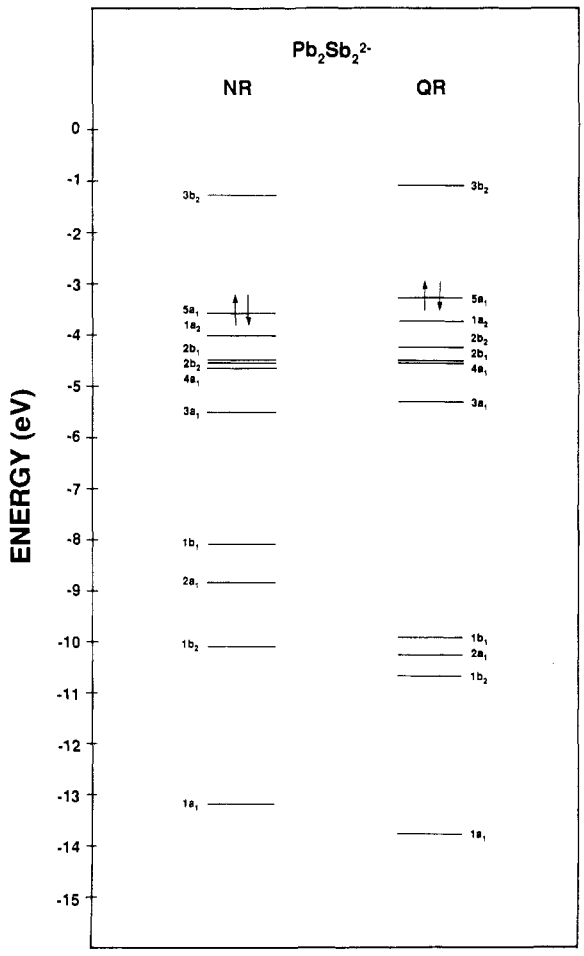


**Figure 2.** MO energy level diagram of the nonrelativistic (NR) and quasi-relativistic (QR) valence ground-state orbital energies (in eV) in the $Pb_2Sb_2^{2-}$ anion.

**Table III.** SW-X$\alpha$ Quasi-Relativistic Muffin-Tin Populations for $Pb_2Sb_2^{2-}$ (%)

| | | Pb | | Sb | | extra-atomic | |
|---|---|---|---|---|---|---|---|
| MO | $-E^a$ | s | p | s | p | int | out |
| $3b_2$ | 1.064 | | 5 | 2 | 38 | 23 | 25 |
| $5a_1$[b] | 3.261 | 0 | 54 | 0 | 6 | 28 | 10 |
| $1a_2$ | 3.719 | | 20 | | 45 | 24 | 7 |
| $2b_2$ | 4.234 | | 29 | 1 | 40 | 22 | 6 |
| $2b_1$ | 4.500 | 4 | 21 | | 40 | 22 | 6 |
| $4a_1$ | 4.534 | 3 | 19 | 0 | 50 | 20 | 6 |
| $3a_1$ | 5.302 | 2 | 17 | 2 | 60 | 8 | 8 |
| $1b_1$ | 9.912 | 81 | 2 | | 5 | 8 | 2 |
| $2a_1$ | 10.236 | 52 | 2 | 30 | 5 | 8 | 2 |
| $1b_2$ | 10.677 | | 3 | 82 | 2 | 9 | 1 |
| $1a_1$ | 13.775 | 31 | 6 | 54 | 6 | 0 | 0 |

[a] MO eigenvalues (eV). [b] Highest occupied MO.

energy level diagrams of the occupied ground-state valence MO's and the first virtual MO at the nonrelativistic (NR) and quasi-relativistic (QR) levels of theory. Focusing our attention on the differences between the NR and QR calculated MO energies, we can immediately see a number of large shifts of the QR energy levels relative to their NR counterparts. The four lowest energy valence MO's for $Sn_2Bi_2^{2-}$ and $Pb_2Sb_2^{2-}$ ($1a_1$, $1b_2$, $2a_1$, and $1b_1$) are all lowered in energy by the QR corrections. The lowering of these energy levels is generally indicative that large contributions of atomic s orbital character are present. This is confirmed by the calculated muffin-tin charge distributions for $Sn_2Bi_2^{2-}$ (Table II) and $Pb_2Sb_2^{2-}$ (Table III). Also, in both anions the $1a_1$ and the $2a_1$ MO's are admixtures of the two symmetric combinations of the atomic s orbitals, as seen in the MO populations. The effect

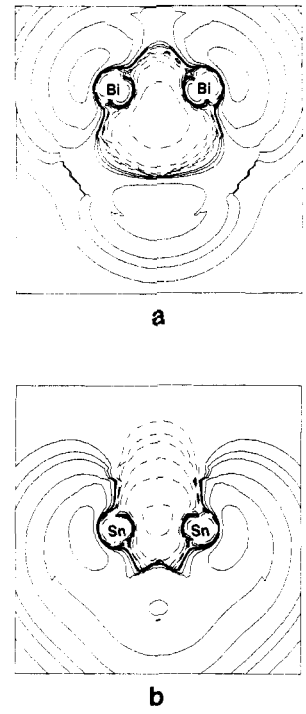


**Figure 3.** Wave function contour plots of the $3a_1$ (a) and $5a_1$ (b) MO's in $Sn_2Bi_2^{2-}$ (contour values: ±0.5, ±0.4, ±0.3, ±0.2, ±0.1, ±0.05, ±0.02, ±0.01, ±0.005, ±0.0035, ±0.002 e/bohr$^3$).

is larger in $Pb_2Sb_2^{2-}$ than it is in $Sn_2Bi_2^{2-}$. This is due to the fact that relativistic corrections lower the energy of the symmetric combination of the Pb 6s AO's ($2a_1$) and reduce the energy difference between it and the symmetrical combination of the Sb 5s AO's ($1a_1$). In $Sn_2Bi_2^{2-}$ the energy of the symmetric combination of the Bi 6s AO's ($1a_1$) is lowered significantly by the relativistic corrections, while the symmetric combination of the Sn 5s AO's ($2a_1$) is lowered only slightly. The net result is that the energy difference between the Bi 6s AO's and the Sn 5s AO's increases, thereby decreasing their interaction relative to the situation found for the $Pb_2Sb_2^{2-}$ anion. Since these interactions are between doubly occupied orbitals, no net bond formation results. The $1b_1$ and $1b_2$ MO's in both anions are the antisymmetric combinations of the same sets of atomic s orbitals discussed above. Relativistic extended Hückel (REX) calculations[24d] on $Sn_2Bi_2^{2-}$ are consistent with the relative ordering and composition predicted by QR SW-X$\alpha$ calculations for these four lower valence MO's.

In both the $Sn_2Bi_2^{2-}$ and the $Pb_2Sb_2^{2-}$ anions the energy difference between the four lowest energy MO's ($1a_1$, $1b_2$, $2a_1$, and $1b_1$) and the next highest MO ($3a_1$), which marks the beginning of the upper valence MO's, is large, especially at the QR level ($\sim$3 and $\sim$4 eV for $Sn_2Bi_2^{2-}$ and $Pb_2Sb_2^{2-}$, respectively). These large energy separations effectively exclude the mixing of the lower valence MO's with the upper valence MO's, making the lower valence MO's pseudo inner-shell lone pairs. The skeletal bonds are therefore formed from the valence atomic p orbitals. This conclusion is substantiated by the MO population analysis of the upper valence MO's for $Sn_2Bi_2^{2-}$ and $Pb_2Sb_2^{2-}$ (Tables II and III). The exclusive participation of the valence p AO's in the formation of the skeletal bonds in Zintl anions has been discussed elsewhere.[1a,23] Wave function plots of two of the upper valence or bonding MO's ($3a_1$ and $5a_1$) for $Sn_2Bi_2^{2-}$ are presented in Figure 3. Figure 3a is the $3a_1$ MO plotted in the mirror plane containing the two Bi atoms. It is clear from this contour plot that the dominant orbitals involved in this bonding MO are Bi 6p AO's. This is also plainly seen in the population analysis (Table II). Figure 3b is the $5a_1$ MO, which is the highest occupied MO (HOMO), plotted in the mirror plane containing the two Sn atoms. This MO is dominantly Sn-based, which is clear from the wave function plot and the MO populations (Table II). The utilization of Sn 5p AO's, which are directed mainly along the Sn–Sn in-

ternuclear axis, is clearly seen in this plot. REX calculations[24d] on the $Sn_2Bi_2^{2-}$ anion yielded a similar result for the composition of the HOMO, which was ~76% Sn 5p and ~4% Sn 5s character. These quantities compare reasonably well with the muffin-tin populations for $5a_1$, which are ~53% for the Sn 5p and ~0% for Sn 5s characters. In general, the lower bond-forming MO's in $Sn_2Bi_2^{2-}$ contain larger contributions from the valence p AO's of the more electronegative Bi atoms, while the p AO character of the more electropositive Sn atoms pervades the higher occupied bonding MO's. A similar effect occurs for the $Pb_2Sb_2^{2-}$ anion. On the basis of our theoretical analysis, the localized valence structure of $Sn_2Bi_2^{2-}$ and $Pb_2Sb_2^{2-}$ is consistent with six two-center, two-electron bonds localized along the edges of the pseudotetrahedron and four inner-shell lone-pair orbitals (i).

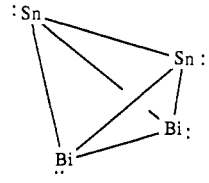


i

Another interesting facet of the electronic structure common to both the $Sn_2Bi_2^{2-}$ and the $Pb_2Sb_2^{2-}$ anions is the lowest unoccupied molecular orbital (LUMO). For both anions the LUMO is the $3b_2$ MO and is antibonding with respect to the two more electronegative atoms (Bi and Sb) and is well-localized on them. A two-electron reduction of the electronically similar $Si_4^{4-}$ anion, which has $T_d$ symmetry,[31] would yield the $Si_4^{6-}$ anion:[32]

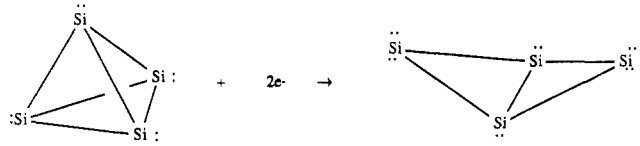


ii iii

The latter anion is known[32] to be a bicyclic "butterfly"-shaped species having $C_{2v}$ symmetry. During the "reduction" process one of the Si–Si bonds in $Si_4^{4-}$ is cleaved, forming the bicyclic $Si_4^{6-}$ anion. Also, a recent paper suggests that the 2e reduction of $P_4$ would yield the similar "butterfly" anion $P_4^{2-}$[21] and not a $D_{4h}$ planar anion.[25] Therefore, if the $3b_2$ MO in either the $Sn_2Bi_2^{2-}$ or the $Pb_2Sb_2^{2-}$ anion was to become occupied (i.e. via a two-electron reduction), the bond between the more electronegative atoms would be cleaved, leaving a bicyclic anion much like $Si_4^{6-}$. The nature of the LUMO in these compounds is also an important point to consider when the electronegativity differences between the constituent atoms increase. If the electronegativity differences between the two types of atoms become large enough, then the HOMO, which we and others[24d] have shown to be based predominantly on the more electropositive atoms, will become higher in energy than the LUMO, which is based predominantly on the more electronegative atoms. A species like the $Tl_2Te_2^{2-}$ anion is a likely representative of this limit of disparity between the AO energies and overlap of the constituent atoms. The interchange of the anticipated $a_1$ HOMO with the $b_2$ LUMO would result in the loss of the Tl–Tl bond and the cleavage of the Te–Te bond, thus unfolding the tetrahedron. This kind of intuition clearly leads to an understanding as to why the $Tl_2Te_2^{2-}$ anion does not have a tetrahedral structure. However, it does not provide any understanding of the final equilibrium geometry.

**$Tl_2Te_2^{2-}$.** We begin our analysis of the electronic structure of the $Tl_2Te_2^{2-}$ anion by examining the role of the Tl 5d and 6s and the Te 5s AO's in the bonding. The MO's derived from these

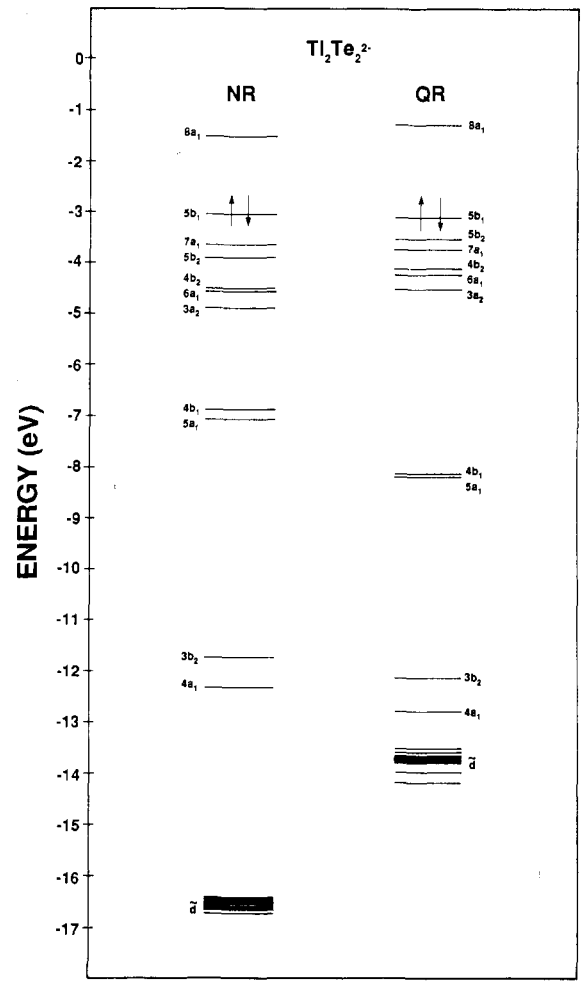


**Figure 4.** MO energy level diagram of the nonrelativistic (NR) and quasi-relativistic (QR) valence ground-state orbital energies (in eV) in the $Tl_2Te_2^{2-}$ anion.

**Table IV.** SW-X$\alpha$ Quasi-Relativistic Muffin-Tin Populations for $Tl_2Te_2^{2-}$ (%)

| | | Tl | | | Te | | extra-atomic | |
|---|---|---|---|---|---|---|---|---|
| MO | $-E^a$ | s | p | d | s | p | int | out |
| $8a_1$ | 1.268 | 0 | 26 | 0 | 0 | 13 | 39 | 20 |
| $5b_1$[b] | 3.133 | 8 | 11 | 2 | | 56 | 16 | 6 |
| $5b_2$ | 3.552 | | 2 | 2 | 0 | 74 | 16 | 6 |
| $7a_1$ | 3.752 | 6 | 24 | 1 | 0 | 41 | 16 | 9 |
| $4b_2$ | 4.127 | | 14 | 3 | 0 | 67 | 8 | 6 |
| $6a_1$ | 4.252 | 1 | 10 | 1 | 0 | 56 | 26 | 5 |
| $3a_2$ | 4.515 | | 19 | 2 | | 62 | 14 | 3 |
| $4b_1$ | 8.170 | 66 | 0 | 1 | | 12 | 8 | 1 |
| $5a_1$ | 8.201 | 61 | 1 | 0 | 12 | 16 | 7 | 2 |
| $3b_2$ | 12.155 | | 3 | 19 | 74 | 0 | 3 | 1 |
| $4a_1$ | 12.800 | 10 | 2 | 20 | 64 | 0 | 3 | 1 |

[a] MO eigenvalues (eV). [b] Highest occupied MO.

AO's are the 14 lowest valence MO's shown in Figure 4. The lowest energy set of MO's is the Tl 5d band. In the NR calculation these orbitals do not interact with any other Tl or Te orbitals. When the relativistic corrections are applied, the entire 5d band is raised ~3 eV in energy. This has the effect of bringing the Tl 5d AO's close enough in energy to mix with the two Te 5s based MO's ($4a_1$ and $3b_2$) (see Table IV). The mixing of the two Te-based MO's with the Tl 5d orbitals of the proper symmetry type causes the 5d band to broaden considerably. Its width in the QR calculation (~0.7 eV) is almost double that of the result in the NR calculation. These interactions are between fully occupied sets of Tl 5d and Te 5s AO's, and no net bonding results. The next two higher energy MO's ($5a_1$ and $4b_1$) are essentially the symmetric and antisymmetric combinations of the Tl 6s AO's.

(31) Schäfer, H.; Janzon, K. H.; Weiss, A. *Angew. Chem., Int. Ed. Engl.* **1963**, *2*, 393.
(32) Eisenmann, B.; Janzon, K. H.; Schäfer, H.; Weiss, A. *Z. Naturforsch, B: Anorg. Chem., Org. Chem., Biochem., Biophys., Biol.* **1969**, *24B*, 457.

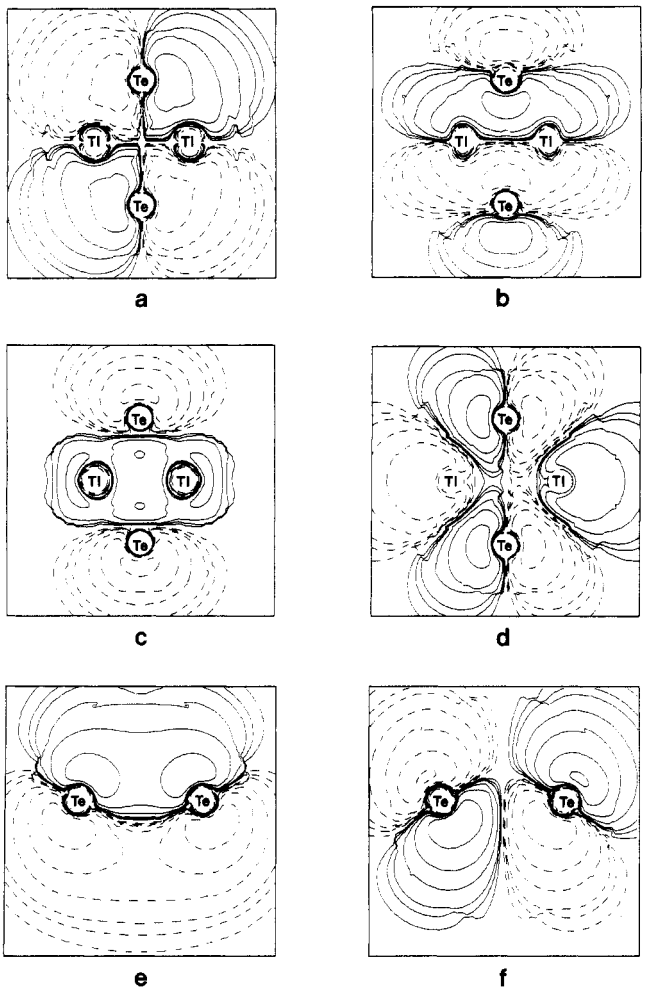


**Figure 5.** Wave function contour plots of the six upper valence MO's in $Tl_2Te_2^{2-}$: (a–d) MO's responsible for the skeletal bonds in the anion ($3a_2$, $4b_2$, $7a_1$, and $5b_1$); (e, f) Te lone-pair orbitals ($6a_1$ and $5b_2$). (The contour values are the same as those listed in Figure 3.)

In addition to Tl 6s character there also exists some contributions from the Te 5s and 5p AO's. We will return to this point later in the discussion; however, we regard these two MO's as more or less nonbonding.

The remaining six upper valence MO's correspond to the four anticipated bonding MO's and the two lone pair or $\pi$ MO's. Wave function plots of these six MO's are presented in Figure 5. Parts a–d of Figure 5 are plotted in a plane that is perpendicular to the $z$ axis and is between the two sets of different atoms (this plane contains the origin of the outer sphere). These four MO's are the $3a_2$, $4b_2$, $7a_1$, and $5b_1$ orbitals, respectively, and correspond to the symmetry types of the four expected valence bonds in this species. The first three of these MO's are obvious bonding combinations between the Tl and Te atoms. The fourth MO ($5b_1$) is clearly antibonding with respect to the Tl and Te atoms. The bonding combinations ($3a_2$, $4b_2$, and $7a_1$) are best described as the donation of Te 5p based AO density into vacant Tl AO's. This is seen in the MO wave function plots (Figure 5a–c) and MO populations (Table IV). It is interesting to note that the lowest energy bonding MO is of $a_2$ symmetry as opposed to the usual $a_1$ symmetry type. The unusual stability of the $3a_2$ MO is due to the fact that the valence MO's are composed of atomic p orbitals and that their interaction is maximized in the $3a_2$ MO by the near-planar geometry of the anion. In fact, the structure of $Tl_2Te_2^{2-}$ does not resemble a square but rather a diamond, with Tl–Tl and Te–Te bond lengths of 3.600 and 4.414 Å, respectively.[14] This structure will tend to maximize the overlaps between the atomic p orbitals in the three bonding MO's ($3a_2$, $4b_2$, and $7a_1$) but will provide for an unfavorable overlap in the $5b_1$ MO. This point is better illustrated by the simple AO interaction diagrams

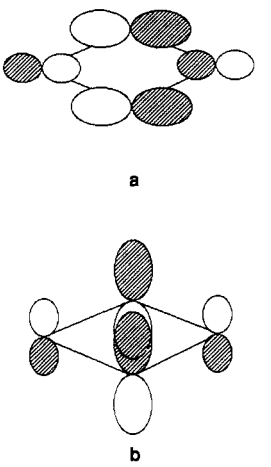


**Figure 6.** Atomic orbital interactions for the $4b_2$ (a) and the $5b_1$ (b) MO's. The larger of the two types of orbitals are the Tl 6p AO's.

presented in Figure 6. Figure 6a shows the phase relationship of the Tl and Te p AO's in the $4b_2$ MO, while Figure 6b shows the phase relationship of the p AO's in the $5b_1$ MO. Due to the geometry of the anion and the spatial extent of the participating orbitals the arrangement of the AO's in Figure 6a will be bonding with respect to the Tl–Te atoms, while the arrangement in Figure 6b will be antibonding.

The origin of the large differences in the two cross-ring distances in the $Tl_2Te_2^{2-}$ anion is only partly due to favorable overlaps in the bonding MO's. An additional electronic factor governs the difference in the two distances. A clearer understanding of this factor may be obtained by viewing the wave function plots of the $6a_1$ and $5b_2$ MO's in Figure 5e,f. These maps were plotted in a plane containing the two Te atoms and the $z$ axis and represent the bonding and antibonding combinations of Te $5p_\pi$ AO's. Thus, the net result is a large repulsive interaction between the two Te atoms. The cellular charge distributions for the $Tl_2Te_2^{2-}$ anion (Table IV) indicate that the majority of the charge density in these two MO's is located in Te 5p AO's, although there is a significant amount of inner-sphere charge density present in the $6a_1$ orbital. These two MO's are the $a_1$ and $b_2$ orbitals of the four-$\pi$-electron system; however, there does not appear to be a large amount of delocalization of these two $\pi$ MO's to the Tl $6p_\pi$ AO's. This is due to the large disparity in energy and overlap between the Te 5p and the Tl 6p AO's. A similar effect[25] also curtails $\pi$ bonding from occurring in the $HgTe_2^{2-}$ anion. The localized nature of the $6a_1$ MO effectively provides no net bonding in this lowest energy $\pi$ MO. These MO's provide two more Te lone-pair orbitals in addition to the two inner-shell Te lone-pair orbitals. However, they occupy stereochemical positions in the coordination spheres of the Te atoms. The bonding in the $Tl_2Te_2^{2-}$ anion may be best thought of as the result of coordination of two $Te^{2-}$ anions by two $Tl^+$ cations. This assumption leads to a prediction of the ground-state orbital configuration of the $Tl_2Te_2^{2-}$ anion which is the same as that predicted by our SW-X$\alpha$ calculations but is different from the orbital configuration found for the classically bonded $Sn_2Bi_2^{2-}$ and $Pb_2Sb_2^{2-}$ anions (the two configurations are related by the interchange of the HOMO and the LUMO). To the extent that the bonding in this species can be represented in a localized fashion, the valence structure iv is reasonably consistent

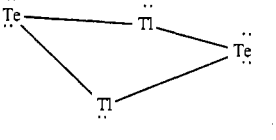


iv

with our calculation. This valence structure has one inner-shell lone pair on each atom and one upper valence lone pair on each Te atom. However, the four bonding orbitals implied in iv are not entirely consistent with the fact that the $5b_1$ MO is not bonding

with respect to the Tl and Te atoms. If the $Tl_2Te_2^{2-}$ anion were to undergo a 2e reduction, then a Tl–Tl trans-ring bond might form, since the LUMO in $Tl_2Te_2^{2-}$ is $8a_1$ and is very likely to be Tl-based although it can not be deciphered from the cellular charge distribution for that MO.

At this point in our discussion we may characterize the $Tl_2Te_2^{2-}$ anion as having a significant ionic component to the bonding, which was also found[25] to be true for $HgTe_2^{2-}$. Typically the bonding and/or arrangement of atoms in ionic compounds is dominated by Coulombic repulsions, which tend to maximize the distances between the atoms or groups bonded to the central atom. If the $Tl_2Te_2^{2-}$ anion were truly an ionic system, then one would predict the geometry to be planar ($D_{2h}$), which would maximize the distances between atoms with the same formal charge. Yet the structure of the $Tl_2Te_2^{2-}$ anion is puckered—a distortion from the anticipated $D_{2h}$ geometry. It is not very likely that the distortion would occur along the Tl–Tl axis, for this would cause the two Te atoms to move closer together and increase their already repulsive interaction. Equivalently, the Te atoms will prefer to be further apart because their formal charge is twice that of the Tl atoms. Therefore, it is more likely that the distortion from $D_{2h}$ symmetry occurs along the Te–Te axis, shortening the Tl–Tl distance only. The puckering of the $Tl_2Te_2^{2-}$ anion is most likely the result of the repulsive interaction of the antisymmetric combination of the Tl 6s AO's ($4b_1$) and the $b_1$ combination of the Te $5p_x$ AO's ($5b_1$). This interaction in a $D_{2h}$ structure would be minimized by the out-of-plane bending of the Tl atoms to a $C_{2v}$ structure. In order to test this hypothesis, we have performed SW-X$\alpha$ QR calculations at a $D_{2h}$ geometry.[33] The calculated charge distributions for the $4b_1$ and $5b_1$ MO's in the $D_{2h}$ geometry are the same as those calculated at the $C_{2v}$ geometry to within 1%. However, the $4b_1$–$5b_1$ orbital energy difference increases by ~0.4 eV. This is a clear indication of increased interaction between these two orbitals. In fact, the $4b_1$ MO is actually lower in energy than $5a_1$ (which is the symmetric combination of the Tl 6s AO's) in the planar structure. Confirmation of this effect awaits a structural analysis by a MO method that has a rigorously defined and meaningful total energy.

(33) The $D_{2h}$ geometry was constructed by bending the Tl atoms in the $C_{2v}$ geometry about the Te–Te axis until all four atoms resided in the same plane. This procedure maintained the original values of the Te–Te and Tl–Te distances. The atomic sphere radii were the same values used in the $C_{2v}$ calculation. The outer sphere and the Watson sphere was subsequently readjusted to be at the center of the anion and to be tangent to the outermost atomic sphere. This calculation was carried out with the $C_{2v}$-symmetry basis set in order to facilitate our analysis.

## Conclusions

The SW-X$\alpha$ method employing quasi-relativistic corrections has been used to study the bonding in the 20-electron tetranuclear heteroatomic Zintl anions $Sn_2Bi_2^{2-}$, $Pb_2Sb_2^{2-}$, and $Tl_2Te_2^{2-}$. The $Sn_2Bi_2^{2-}$ and $Pb_2Sb_2^{2-}$ anions, which both have pseudotetrahedral geometries, have ground-state orbital configurations consistent with a localized valence structure having two-center, two-electron bonds along the six edges of the tetrahedron and one valence lone pair on each atom. The bonding MO's are formed almost entirely from the p AO's on the constituent atoms, while the lone-pair MO's are formed from the valence s AO's and are inert electron pairs. The HOMO's in these two anions are composed primarily of atomic p orbitals of the more electropositive atoms. The LUMO's of the two anions are localized primarily on the more electronegative atoms and are antibonding with respect to them. If the electronegativity differences between the two different atoms become large enough, as in the $Tl_2Te_2^{2-}$ anion, then the HOMO and the LUMO of the chemically bonded anions will interchange, giving a different orbital configuration and cleaving the two homonuclear bonds. The bonding in the $Tl_2Te_2^{2-}$ anion is best described as the result of coordination of two $Te^{2-}$ anions with two $Tl^+$ cations. This view of the bonding leads to the correct prediction of the ground-state orbital configuration for the anion. Of the four predicted bonding MO's, only three are actually bonding. As for the $Sn_2Bi_2^{2-}$ and $Pb_2Sb_2^{2-}$ anions, the valence atomic s orbitals on the Tl and Te atoms are doubly occupied and are essentially inert. Two additional Te lone-pair orbitals were found. They are formed from the bonding and antibonding combinations of the two Te $5p_\pi$ type AO's. Their interaction is repulsive and is probably responsible for the Te–Te trans-ring distance being longer than the corresponding Tl–Tl distance. Due to the large ionic component to the bonding the $Tl_2Te_2^{2-}$ anion should be planar; however, a repulsive interaction between the antisymmetric combination of the Tl 6s AO's and the $b_1$ combination of the Te 5p AO's may be responsible for the distortion of the two Tl atoms out of plane.

**Acknowledgment.** We thank the Robert A. Welch Foundation (Grant Y-743) and the Organized Research Fund of the University of Texas at Arlington for their support of this work.

**Registry No.** $Sn_2Bi_2^{2-}$, 113251-42-6; $Pb_2Sb_2^{2-}$, 113273-58-8; $Tl_2Te_2^{2-}$, 77321-80-3.

Contribution from the Department of Chemistry, Clemson University, Clemson, South Carolina 29634-1905

# Reaction of Certain Nitrogen Oxides with Iron(III) Porphyrin $\mu$-Oxo Complexes

Marc F. Settin and James C. Fanning*

*Received February 24, 1987*

The nitrogen oxides NO, $N_2O_4$, and $N_2O_3$ and the $\mu$-oxo complexes $[Fe(TPP)]_2O$ and $[Fe(OEP)]_2O$, where TPP and OEP are the dianions of *meso*-tetraphenylporphine and octaethylporphyrin, respectively, were reacted in toluene in the absence of $O_2$. $[Fe(TPP)]_2O$ was reacted with the nitrogen oxides in dimethylacetamide (DMA). All of the reactions were followed by changes in the electronic spectra. The NO reaction with $[Fe(TPP)]_2O$ in toluene yielded a solid product, $Fe(TPP)(NO)(NO_2)\cdot C_7H_8\cdot 2H_2O$. The $N_2O_4$ and the $N_2O_3$ reactions in toluene produced $Fe(TPP)NO_3$ and $Fe(OEP)NO_3$, while in DMA these reactions gave an equilibrium amount of $Fe(TPP)(DMA)_x^+$, the solvated complex.

## Introduction

For many years studies of iron porphyrin oxynitrogen complexes have been limited to only a variety of nitrosyl hemes.[1-6] A few years ago the nitrate complexes $Fe(TPP)NO_3$ and $Fe(OEP)NO_3$ were prepared and studied.[7] Recently the nature of $Fe(TPP)NO_2$, $Fe(TPP)(NO_2)_2^-$, and $Fe(OEP)(NO_2)_2^-$ has been examined in solution.[8] These types of complexes may be part of a number of processes, such as those involving nitrate and nitrite reductase

(1) Wayland, B. B.; Olson, L. W. *J. Am. Chem. Soc.* **1974**, *96*, 6037.
(2) Lancon, D.; Kadish, K. M. *J. Am. Chem. Soc.* **1983**, *105*, 5610.
(3) Bazylinski, D. A.; Holocher, T. C. *J. Am. Chem. Soc.* **1985**, *107*, 7982.
(4) Hille, R.; Olson, J. S.; Palmer, G. *J. Biol. Chem.* **1979**, *254*, 12110.
(5) Louro, S. R. W.; Ribeiro, P. C.; Bemski, G. *Biochim. Biophys. Acta* **1981**, *670*, 56.
(6) Chien, J. C. W. *J. Am. Chem. Soc.* **1969**, *91*, 2166.
(7) Phillipi, M. A.; Baeziger, N.; Goff, H. M. *Inorg. Chem.* **1981**, *20*, 3904.
(8) Fernandes, J. B.; Feng, D.; Chang, A.; Keyser, A.; Ryan, M. D. *Inorg. Chem.* **1986**, *25*, 2606.

0020-1669/88/1327-1431$01.50/0 